

REPORT DOCUMENTATION PAGE

Form Approved
OMB No. 0704-0188

Public reporting burden for this collection of information is estimated to average 1 hour per response, including the time for reviewing instructions, searching existing data sources, gathering and maintaining the data needed, and completing and reviewing the collection of information. Send comments regarding this burden estimate or any other aspect of this collection of information, including suggestions for reducing this burden to Washington Headquarters Services, Directorate for Information Operations and Reports, 1215 Jefferson Davis Highway, Suite 1204, Arlington, VA 22202-4302, and to the Office of Management and Budget, Paperwork Reduction Project (0704-0188), Washington, DC 20503

| | | | |
|--|---|--|---|
| 1. AGENCY USE ONLY (Leave Blank) | | 2. REPORT DATE June 28, 2004 | 3. REPORT TYPE AND DATES COVERED Final (2/20/02 - 3/31/04) |
| 4. TITLE AND SUBTITLE Sound speed and attenuation measurements in unconsolidated glass bead sediments saturated with viscous pore fluids | | | 5. FUNDING NUMBERS N00014-02-1-0336 |
| 6. AUTHOR(S) Brian T. Hefner and Kevin L. Williams | | | 8. PERFORMING ORGANIZATION REPORT NUMBER |
| 7. PERFORMING ORGANIZATION NAME(S) AND ADDRESS(ES) Applied Physics Laboratory University of Washington 1013 NE 40th St. Seattle, WA 98105-6698 | | | |
| 9. SPONSORING/MONITORING AGENCY NAME(S) AND ADDRESS(ES) Office of Naval Research 800 N. Quincy St. Arlington, VA 22217-5660 Attn: Dr. Ellen Livingston, Code 3210A | | | 10. SPONSORING/MONITORING AGENCY REPORT NUMBER |
| 11. SUPPLEMENTARY NOTES Report has been submitted for publication in the <i>Journal of the Acoustical Society of America</i> | | | |
| 12a. DISTRIBUTION/AVAILABILITY STATEMENT Approved for public release | | | 12b. DISTRIBUTION CODE |
| 13. ABSTRACT (Maximum 200 words) During the sediment acoustics experiment (SAX99) independent sound speed and attenuation measurements were made in a well-characterized sandy sediment. These measurements covered a broad frequency range that made it possible to test both Biot theory and Buckingham's more recent grain-to-grain attenuation model. Biot theory was able to model sound speed well but was unable to predict attenuation measured above 50 kHz. A series of measurements was made in the laboratory to test the hypothesis that this modeling deviation was due to scattering within the sediment. The measured attenuation in the glass bead sediments exhibited the same frequency dependence observed in the SAX99 data, indicating that scattering is not the relevant attenuation mechanism. A sediment model is proposed which is a hybrid of the Biot and Buckingham theories. This hybrid model is able to predict both attenuation and sound speed in the SAX99 sediment and in the laboratory sediments. The implications of the success of the hybrid model are discussed. | | | |
| 14. SUBJECT TERMS acoustic attenuation, sandy sediments, scattering, Biot-Stoll theory, Buckingham's model | | | 15. NUMBER OF PAGES 29 |
| | | | 16. PRICE CODE |
| 17. SECURITY CLASSIFICATION OF REPORT Unclassified | 18. SECURITY CLASSIFICATION OF THIS PAGE Unclassified | 19. SECURITY CLASSIFICATION OF ABSTRACT Unclassified | 20. LIMITATION OF ABSTRACT UL |

20040806 053

**Sound speed and attenuation measurements in
unconsolidated glass bead sediments saturated with
viscous pore fluids.**

Brian T. Hefner and Kevin L. Williams

*Applied Physics Laboratory
College of Ocean and Fisheries Sciences
University of Washington
1013 N.E. 40th Street
Seattle, WA 98195*

Submitted: June 28, 2004

Running Title: Sound propagation in glass bead sediments.

Abstract

During the sediment acoustics experiment (SAX99), a number of independent sound speed and attenuation measurements were made in a well-characterized sandy sediment. These measurements covered a broad frequency range and made it possible to test both Biot theory and Buckingham's more recent grain-to-grain attenuation model. While Biot theory was able to model the sound speed well, it was unable to predict the attenuation measured above 50kHz. This paper presents a series of measurements made in the laboratory on a simple glass bead sediment to test the hypothesis that this deviation was due to scattering within the sediment. The sediments used were saturated with two fluids with different viscosities in order to shift the dispersion into the frequency range of the measurement system. The measured attenuation in the glass bead sediments exhibited the same frequency dependence as observed in the SAX99 data indicating that scattering is not the relevant attenuation mechanism. A sediment model is proposed which is a hybrid of Biot and Buckingham's theories. This hybrid model is able to model both the attenuation and sound speed in the SAX99 sediment and in the laboratory sediments. The implications of the success of this hybrid model are also discussed.

PACS numbers: 43.30.Ma, 43.20.Jr

I. INTRODUCTION

In the study of sediment acoustics, there is an ongoing debate about the nature of dispersion and attenuation in unconsolidated, sandy sediments. Many measurements have been made in sandy sediments, both in situ and in the laboratory, as well as in simpler unconsolidated glass bead sediments. The results of these experiments have led to two differing conclusions. Some measurements seem to indicate that attenuation in these sediments varies as the first power of the frequency, f^1 , with little or no significant dispersion. This view has found its most vocal support in Hamilton¹ and has recently been revisited by Buckingham who argues that this conclusion is supported by current research into the properties of dry sand²⁻⁴. Both Hamilton and Buckingham have argued that the sediment is best described by a viscoelastic model. Both of these approaches determine the relevant parameters through empirical fits to the data limiting their predictive value⁵. The approaches differ, however, in that Hamilton's approach is purely empirical while Buckingham believes that the attenuation is due to friction between the sand grains⁴. Buckingham feels that the relevant parameters can be determined from the fluid and sand properties although it is not clear at this point in the theory's development how this would be done.

Due to the porous nature of the sediment, some researchers feel that the relative motion of the pore fluid and the sediment frame should lead to viscous damping of the acoustic wave. Biot theory provides a successful description of sound propagation through porous materials^{6,7} and has thus been applied to modeling sand sediments. The attenuation predicted by Biot theory, however, varies as f^2 at low frequencies and $f^{1/2}$ at high frequencies which contradict some of the measurements in sandy sediments. The sound speed is also predicted to exhibit significant dispersion in the frequency range where the transition between these two limiting attenuations takes place. Some researchers, most notably Stoll⁸, note that there are deviations from the f^1 frequency dependence in many measurements as well as evidence of dispersion indicating that viscous losses due to the motion of the pore fluid may be important. Indeed, many measurements have been successfully modeled with Biot theory by assuming complex frame moduli to account for friction and local viscous flow at the grain contacts. This modified theory has come to be known as Biot-Stoll theory⁹. Biot theory has an advantage over the viscoelastic models of Hamilton and Buckingham

in that the relevant parameters in the theory can in principle be measured, although not without some effort. Biot-Stoll theory remains empirically driven, however, in that the complex frame moduli are generally determined from a best fit to the data.

With the number of measurements available, it might seem strange that a consensus has not been reached on the proper description of sound propagation in sediments. The problem lies not with a lack of experimental effort but rather in the difficulties inherent in performing these measurements. Usually it not possible to make sound speed and attenuation measurements over a frequency range broad enough to observe the dispersion predicted by Biot-Stoll theory nor is it usually possible to fully characterize the sediment. Realizing the importance of overcoming these difficulties, a number of researchers, utilizing different measurement techniques, came together to determine both the sound speed and attenuation in the sediment at a single site during a recent high-frequency sediment acoustics experiment (SAX99)^{10,11}. Extensive efforts were made to determine the properties of the sediment and several researchers measured the sound speed in the sediment over a frequency range of 125Hz-400kHz and attenuation over a frequency range of 2.6-400kHz. Details of these measurements can be found in Ref. 12.

Despite the broad range of frequencies and careful measurement of the sediment properties, the results of the SAX99 experiments have not been successful in resolving the sediment acoustics debate. Both Biot-Stoll theory and Buckingham's model have been applied to the data and both have their respective strengths and weaknesses as shown in Fig. 1. Biot-Stoll theory captures the dispersion in the sound speed across most of the frequencies with the exception of the two lowest frequency measurements. The measured attenuation deviates, however, from that predicted by Biot-Stoll theory at the highest frequencies and appears to follow the f^1 frequency dependence observed previously. Consequently, Buckingham's model fits the attenuation well at these high frequencies with only a slight deviation from the lower frequency measurements. His theory is not as successful in modeling the sound speed as it predicts a curvature in the dispersion that is opposite that of the measured values and only fits the data over a limited frequency range.

As Williams et. al.¹² points out, these results are one of four separate measurements that indicate that the sound speed in sand sediments at low frequencies is lower than at

high frequencies. This is consistent with the predictions of Biot and the authors speculate that the deviation in attenuation at high frequencies may be due to scattering within the sediment from either volume inhomogeneities or shell and shell fragments. In order to test this hypothesis, a series of laboratory measurements were made in simple glass bead sediments. The measurements were performed using one of the systems which was used during SAX99 to measure sound speed and attenuation over the 100-260 kHz frequency range. Although this range was extended down to 60 kHz for the laboratory experiments, it is still not low enough to observe significant dispersion for glass beads saturated with water. To overcome this limitation, a second glass bead sediment was saturated with Silicone oil which has a viscosity of approximately 0.1 Pa.s. Biot theory predicts that by increasing the viscosity, the region of significant dispersion should shift upward in frequency and hence should be observable with the measurement system. Details of the sediments as well as the measurement system are discussed in Section II. This experiment is similar to the measurements made by Seifert et.al.¹³ In those measurements, several different fluids were used to vary the viscosity of the pore fluid from 0.001 to 1 Pa.s. However, they observed an f^2 frequency dependence in the attenuation whereas the measurements presented here show an f^1 dependence over a similar range of frequencies. For the measurements in a silicone oil saturated sediment, significant dispersion is observed in the current experiments. These results are similar to those of SAX99 in that the attenuation deviates from Biot theory over the same frequency range while the sound speed is well described by Biot theory. The measurement results and model comparisons are shown in Section III. These results do not support the scattering hypothesis for the SAX99 results and while neither Biot nor Buckingham's theory individually captures all aspects of the data, a model which combines the important aspects of both is able to describe all three data sets. This model is developed in Section IV while the implications of the data-model comparisons using this hybrid model are discussed in Section V.

II. EXPERIMENTAL PROCEDURE

The system used to make the measurements described here was deployed during SAX99 by APL-UW.^{10,12} This diver-deployed system was known as the 'attenuation array' and

was able to make sound speed measurements in the 100-200 kHz frequency range and attenuation measurements in the 100-260 kHz frequency range. The system consists of four ITC 6148 transducers (two receivers and two transmitters) which allowed measurements to be made over four separate paths. During the experiment the path lengths were from 22 to 44 cm and the transducers were inserted into the sediment to a depth of 10 cm. Because this system was designed to be diver-deployed, it was relatively compact and thus easy to use for laboratory based measurements.

The sediments in the laboratory measurements were composed of well-sorted glass beads which had diameters in the range of 0.43 to 0.30 mm and a minimum roundness of 90%. Two fluids were used to saturate the glass beads: water and a silicone oil with a viscosity of 0.098 Pa·s. Biot theory predicts that by increasing the viscosity of the pore fluid, the dispersion in the sound speed should shift to higher frequencies⁷. By shifting the dispersion up in frequency, it should be observable in the frequency range of the attenuation array. It should also provide a second test of Biot theory in that the attenuation should scale with the viscosity of the pore fluid. In the measurements of Seifert et. al. this scaling was not observed leading them to reject Biot's porous medium description of the unconsolidated sand sediment¹³.

In order to insure that bubbles would not be present in the sediments, a vacuum was applied to the fluid before the sediment was added and allowed to degas over several days. In order to withstand the vacuum, two stainless steel oil drums were chosen as tanks for the sediments. These drums had an inner diameter of 54.6 cm and a depth of 83.5 cm. The glass beads were added to the degassed fluids in 10 cm layers and the glass bead/fluid combination was degassed and then stirred after each layer was added. Over the course of the experiments, the sediments were stirred and a vacuum was applied to the tanks periodically to remove any bubbles that may have formed. The glass bead/water sediment had a depth of 37 cm with a water layer above it that was 36 cm thick. The glass bead/Silicone oil sediment had a depth of 23 cm with a 22 cm thick layer of Silicone oil above it.

The properties of each sediment, including that of SAX99, are given in Table 1. The bulk modulus and density of the glass beads were provided by the manufacturer, Potters

Industries Inc., and are consistent with reported values of glass found in the literature. The bulk modulus of the water was determined from the average sound speed measurement in the water. The density and viscosity of the Silicone oil was provided by the manufacturer, Silchem, and the bulk modulus of the oil was determined from its measured sound speed.

The remaining properties important for the application of Biot theory and which are often difficult to measure in sand sediments are the porosity, β , permeability, κ , and the tortuosity, α . The permeability of the glass bead/water sediment was determined by taking samples of the sediment with a known volume and measuring the density before and after removing the water by drying the sample in an oven. The value of 0.384 is reasonably close to the random close packing limit for identical spheres. The same procedure could not be applied to the Silicone oil sediment because the vapor pressure of the oil is much higher than that of water. The random close packed limit of 0.36 was assumed here instead. It may seem reasonable to assume that the porosity should be the same in both cases, but this assumption was rejected because the macroscopic properties of the sediments were found to be much different. The Silicone oil sediment was found to heal much faster than the water sediment when stirred or when transducers were inserted and removed from the sediment. Also, during degassing, bubbles were able to move out from the interior of the silicone oil sediment much faster and easier than from the water saturated sediment. It is hypothesized that this is due to the higher viscosity of the silicone oil which allows the beads to slide relative to one another with less friction due to hydrodynamic lubrication¹⁴. It seems more likely that the beads are able to reach a denser ground state in Silicone oil than they would be able to in water.

The hydraulic permeability was calculated using the Kozeny-Carmen relation¹⁵,

$$\kappa = \frac{\beta^3 d^2}{180 (1 - \beta)^2}, \quad (1)$$

where d is the average diameter of the glass beads. This relationship was tested for the water/glass bead sediment using a constant head permeameter and the value calculated using the Kozeny-Carmen relation was found to fall within the error of the measurement. A measurement of the tortuosity is notoriously difficult to make for unconsolidated sediment and as a result an expression derived by Berryman for a collection of spheres was used¹⁶.

The expression,

$$\alpha = \frac{2}{1 + \beta}, \quad (2)$$

relates the tortuosity to the porosity and gives a lower value than the expression that was used previously by Berryman to describe sintered glass bead packs¹⁷. As Berryman shows in Table 1 of Ref. 16, the expression given in Eq. 2 fits the analytical values for ordered unconsolidated glass bead packs whereas the previous expression is a better fit to sintered glass bead packs. As a result, Eq. 2 is used for the tortuosities of the glass bead sediments.

Because the diameter of the tanks were smaller than the original attenuation array, the array was reconfigured for use in the tanks. The new arrangement maintained the original electronics and transducer mounts, while repositioning the transducers such that they sat at the corners of a rectangle. For each transmitter, one receiver was mounted close to provide a short path length, while the second transducer was mounted further away to provide a longer path length. The sound speed was determined using the difference in phases between a pulse received at two different transducers¹⁸. As a result, the difference in path lengths, ΔP , is the important distance for this measurement. For the water/glass bead sediment $\Delta P_1 = 25.99$ cm and $\Delta P_2 = 25.95$ cm while for the silicone oil/glass bead sediment $\Delta P_1 = 14.39$ cm and $\Delta P_2 = 14.97$ cm. The reduction in path length for the silicone oil was necessary in order to overcome the signal loss due to the increased attenuation. The attenuation was determined from the spectral amplitudes using the method described in Ref. 18. This technique also depends on the difference in the two path lengths. The sound speed and attenuation measurements for both sediments were performed using the original attenuation array over a frequency range of 100 kHz to 260 kHz. However, due to the large attenuation, measurements above 200 kHz could not be made in the silicone oil saturated sediment.

For each measurement, the transducers were first placed in the overlying fluid layer and the sound speed and spectral amplitude of the pulse in the fluid were measured. The transducers were then inserted into the sediment. The depth of the transducers in the water/glass bead sediment was 10 cm while in the silicone oil/glass bead sediment it was 11.4 cm. The tank was then shaken by hand for approximately two minutes then allowed to sit for 4-6 hours to allow the sediment to settle. The sound speed and spectral amplitude

were then measured and after the transducers were removed from the sediment, the sound speed and spectral amplitudes in the fluid were again measured. Once the transducers were removed from the tank, the sediment was again shaken and allowed to settle overnight.

In order to extend the lower limit of the frequency range of the array, a Reson TC4040 was introduced which was able to operate in the 60 kHz to 100 kHz range. The difference in path length for the new array was $\Delta P_1 = 7.82$ cm in water and $\Delta P_1 = 4.53$ cm in silicone oil. Unfortunately, there was an unresolved problem with the phase of the output pulse of the new array which produced an offset in the measured sound speed. Consequently these phase speed measurements were discarded. The attenuation measurements were unaffected by this problem and are presented here.

III. RESULTS AND MODEL-DATA COMPARISONS

The sound speed ratio and attenuation measured in each sediment are presented in Fig. 2. Each data point is the mean of measurements of approximately 20 realizations of the each sediment. The error bars on each data point reflect the uncertainties in the path lengths as well the distribution of the measured values. As predicted by Biot theory, the sound speed in the silicone oil/glass bead sediment exhibits greater dispersion than the water/glass bead sediment. However, contrary to Biot theory, both media show a frequency dependence for the attenuation that is greater than $f^{1/2}$. A linear fit to the attenuation shows that the attenuation follows an $f^{1.06}$ dependence for the water/glass bead sediment and an $f^{0.99}$ dependence for the silicone oil/glass bead sediment.

In order to test Biot theory against this data, it is necessary to know certain material parameters in order to determine the sound speed and attenuation. A majority of these parameters are discussed in the previous section and are given in Table I, but there are two notable exceptions. For both glass bead sediments, the frame bulk modulus, K_b , and the shear modulus, μ , are unknown. Williams has shown that in most sand sediments, because the bulk and shear frame moduli are much smaller than the other moduli, they can be neglected with only minor errors (0.5%) in the high frequency sound speed and attenuation. Taking the $K_b = \mu = 0$ limit of Biot theory yields the effective density fluid model (EDFM) which gives the complex wavenumber for the compressional wave. The

EDFM along with the fluid, solid, and sediment properties in Table I yield the solid lines in Fig. 2. In both sediments, the EDFM captures the measured sound speed values but does not capture the high frequency behavior of the attenuation. Although the EDFM does not capture the details of the attenuation, it does predict an increase in attenuation between the water and silicone oil sediments that is on the same order as the increase in the measured attenuation. Consequently, both the frequency scaling and frequency dependence contradict what was measured by Seifert et. al.¹³

The compressional wavenumber in Buckingham's model can be expressed as⁴

$$k^2 = \frac{\omega^2 \rho}{H + \gamma_T (-i\omega T)^n}, \quad (3)$$

where ω is the radial frequency, $\rho = (1 - \beta)\rho_s + \beta\rho_f$ is the average density of the sediment, $H = (\beta/K_f + (1 - \beta)/K_s)^{-1}$ is the bulk modulus of the sediment evaluated from Wood's equation, $\gamma_T = \gamma_p + 4/3\gamma_s$ is the rigidity coefficient, and m is the material exponent. Note that the rigidity coefficient is a combination of Buckingham's compressional and shear rigidity coefficients. Since there is not a shear wave measurement to use to determine the values of m and γ_s , the rigidity coefficients can be combined into a single constant which must be fit to the data along with the material exponent. Note that the assumption of $m = n$ has also been made.

The sound speed and attenuation given by Buckingham's model are shown as the dashed lines in Fig. 2 and the values of γ_T and m are given in Table I. For the water/glass bead sediment, the values of these parameters are comparable to those determined for the SAX99 data in that m and γ_T are the same order of magnitude. For the silicone oil sediment, m is an order of magnitude larger while γ_T is two orders of magnitude smaller. It may be that the large viscosity of the silicone oil brings into doubt the approximation made in Eq. 58 and 59 in Ref. 4 which stems from the assumption that viscous effects at the grain contacts are negligible. If these approximations are not made, the number of unknowns increases to three (this again assumes that the shear and compressional values are the same), the determination of which is beyond the scope of this paper.

the components of the strain tensor and how they relate to the stresses given by Eq. (4) and (5). Consider first the shear strain in the frame matrix,

$$\epsilon_{ij} = \frac{1}{2}\gamma_{ij} = \frac{1}{2}\left(\frac{\partial u_i}{\partial x_j} + \frac{\partial u_j}{\partial x_i}\right). \quad (6)$$

This strain will produce a shear stress within the matrix due to the translational sliding of the grains against on another. From Eq. (5), the shear stress is

$$\sigma_{ij} = \eta_s h_s(t) \otimes \left\{ \frac{dv_i(t)}{dx_j} + \frac{dv_j(t)}{dx_i} \right\}, \quad (7)$$

where $v_i = \dot{u}_i$. Assuming that the disturbance in the matrix has a harmonic time dependence, $u_i e^{-i\omega t}$, then Eq. (7) becomes

$$\sigma_{ij} = 2\mu_b(\omega) \epsilon_{ij} \quad (8)$$

where

$$\mu_b(\omega) = -i\omega\eta_s H_s^*(i\omega) \quad (9)$$

and $H_s^*(i\omega)$ is the complex conjugate of the temporal fourier transform of $h_s(t)$.

For the second elastic modulus of the granular matrix, consider the response of a unit cube of the matrix to a uniform pressure. This pressure gives rise to a change in the volume of the cube equal to $e = \nabla \cdot \vec{u}$ and will also produce radial sliding at the grain contacts due to the compression of the grains. Using Eq. (4), the stress-strain relation in this situation becomes

$$\sigma = \lambda_p \nabla [h_p(t) \otimes \vec{v}]. \quad (10)$$

Once again assuming a harmonic compression, the stress-strain relation becomes

$$\sigma = K_b(\omega) e, \quad (11)$$

where

$$K_b(\omega) = -i\omega\lambda_p H_p^*(i\omega) \quad (12)$$

and $H_p^*(i\omega)$ is the complex conjugate of the temporal fourier transform of $h_p(t)$. The dynamic elastic moduli of the matrix are therefore the grain-to-grain shear modulus, $\mu_b(\omega)$, and the grain-to-grain bulk modulus, $K_b(\omega)$.

The temporal Fourier transforms of the MIRFS in Eq. (9) and (12) are given approximately by⁴

$$H_s^*(i\omega) \approx \frac{\Gamma(1-m)}{(-i\omega t_s)^{1-m}} \quad (13)$$

and

$$H_p^*(i\omega) \approx \frac{\Gamma(1-m)}{(-i\omega t_p)^{1-m}} \quad (14)$$

where Γ is the complement of the incomplete gamma function, m, n are the material exponents, and $t_{s,p}$ are the stress relaxation time constants. The approximations are valid assuming that $\omega t_{s,p} \ll 1$. With these expressions, the elastic moduli can be written as

$$\mu_b(\omega) = \gamma_s (-i\omega T)^m \quad (15)$$

and

$$K_b(\omega) = \gamma_p (-i\omega T)^n \quad (16)$$

where the shear and compressional rigidity coefficients are

$$\gamma_s = \frac{\eta_s}{t_s} \Gamma(1-m) \left(\frac{t_s}{T}\right)^m \quad (17)$$

and

$$\gamma_p = \frac{\lambda_p}{t_p} \Gamma(1-n) \left(\frac{t_p}{T}\right)^n. \quad (18)$$

The time constant T has been introduced to keep terms raised to the fractional powers n and m dimensionless. The expressions are independent of T and hence it is conveniently taken to be $T = 1s$. These expressions for the frame moduli can be used in Biot's equations. A detailed discussion of Biot's equations can be found in Ref. 9 while a concise presentation is found in Eq. (1)-(8) of Ref. 12. The use of Eq. (15) and (16) in Biot Theory will be referred to as the "Biot-Buckingham model" for the remainder of this paper.

The expressions for the moduli given by Eq. (15) and (16) are not new and were first suggested by Biot in the development of a phenomenological approach to solid dissipation in porous medium^{6,7} and later explored in detail, outside the context of Biot theory, by Kjartansson²⁰. Kjartansson was motivated by early measurements on absorption of sound in rocks which found that the energy lost per cycle or wavelength, Q , was independent of the frequency. To account for this, he proposed a model for the elastic moduli which has essentially the same form as Eq.(15) and (16). For the shear modulus, and likewise for the bulk modulus, the phase angle between the stress and the strain can be determined by rewriting the modulus as

$$\mu_b(\omega) = \gamma_s |\omega T|^m \exp\left(-i \frac{m\pi}{2} \text{sgn}(\omega)\right). \quad (19)$$

The Q is directly related to this phase angle and from this expression for the shear modulus,

$$\frac{1}{Q} = \tan\left(\frac{m\pi}{2}\right). \quad (20)$$

Because of this property, the model is often referred to as the constant Q (CQ) model.

Kjartansson showed that this model could be expressed as an infinite set of viscoelastic Zener elements²⁰. As a consequence of this construction, the CQ model is causal. Buckingham has also shown this directly in the development of his model². The introduction of CQ frame moduli into Biot theory was investigated by Turget²¹ who numerically integrated the Kramers-Krönig relations and also found that this viscoelastic Biot theory was causal.

To examine the properties of this hybrid model, it is easiest to look first at the behavior of the shear wave. In the Biot-Buckingham model, the shear wave number becomes

$$k_s^2 = \omega \frac{\rho_{eff}^{(s)}}{\mu_b(\omega)} \quad (21)$$

where

$$\rho_{eff}^{(s)} = \rho_f \left(\frac{\alpha(1-\beta)\rho_s + \beta(\alpha-1) + \frac{i\rho\beta\eta F(\omega)}{\rho_f \kappa \omega}}{\alpha + \frac{i\beta\eta F(\omega)}{\kappa \omega}} \right). \quad (22)$$

and μ_b is the viscoelastic shear modulus given by Eq. (15). For a detailed derivation of this expression see p. 19 of Ref. 9. All of the constants in $\rho_{eff}^{(s)}$ can be measured directly.

Following Buckingham, the material exponent, m , and the rigidity coefficient, γ_s , can be evaluated given a measurement of the shear speed and attenuation at a single frequency. Writing the shear modulus as

$$\gamma_s (-i\omega T)^m = \gamma_s (\omega T)^m (\cos(m\pi/2) - i \sin(m\pi/2)), \quad (23)$$

the material exponent can then be found from

$$m = \frac{2 \operatorname{Im}(\rho_{eff}^{(s)}/k_s^2)}{\pi \operatorname{Re}(\rho_{eff}^{(s)}/k_s^2)}, \quad (24)$$

and the rigidity coefficient is then

$$\gamma_s = \frac{\omega^2 \rho_{eff}^{(s)}}{(-i\omega T)^m k_s^2}, \quad (25)$$

where $k_s = \omega/c_s - i\alpha_s$, c_s is the shear wave speed, and α_s is the attenuation. During SAX99, the shear wave speed and attenuation were measured¹¹ at 1 kHz and were $c_s = 120$ m/s with a range of 97 to 147 m/s and $\alpha_s = 30$ dB/m with a range of 21 to 40 dB/m. Using these values, the material exponent, m , has a best fit of 0.0506 to the mean sound speed and attenuation. The rigidity coefficient has a best fit of 1.82×10^7 Pa to the mean values of the sound speed and attenuation.

The shear speed and attenuation are shown as the solid lines in Fig. 3. Also shown in this figure are the predictions of the Buckingham model and the predictions of Biot theory with a complex shear modulus with no frequency dependence. For this complex shear modulus, the best fit to the mean values of the sound speed and attenuation is $2.83 \times 10^7 - i2.25 \times 10^6$ Pa.

In Ref. 2, Buckingham attempts to address the question of whether it is necessary to account for viscous losses due to global or local motion of the pore fluid when modeling sound propagation in marine sediments. In order to do this, he introduces viscous loss terms into the equation of motion for the saturated sediment. The solution to the resulting wave equation indicates a frequency dependence for both the sound speed and attenuation from which he is able to draw two conclusions. In the combined model, the intergranular friction appears to dominate at lower frequencies while the pore fluid viscosity dominates at

high frequencies. Also, the sound speed varies with frequency as $f^{1/2}$ in the high frequency regime where the pore fluid viscosity dominates.

In the Biot-Buckingham theory, the effects of both loss mechanisms are not as clear cut as Buckingham's test model. In the low frequency limit, the sound speed varies with frequency as $f^{m/2}$, while the attenuation varies as $f^{2-m/2}$ for $m \ll 1$ and then transitions to $f^{1-m/2}$ as m increases. For the properties of the SAX99 sediment, which are typical of a sandy sediment, this transition occurs for extremely small m and by $m \approx 0.02$ the intergranular friction has become the dominant loss mechanism, as predicted by Buckingham's test model. In the high frequency limit, the shear speed also varies with frequency as $f^{m/2}$. This contradicts Buckingham's test model where the sound speed varied as $f^{1/2}$, indicating that even at high frequencies the intergranular friction remains dominate. For high frequencies, the attenuation also exhibits behavior similar to what was observed at low frequencies. for small m , the attenuation varies with frequency as $f^{1/2-m/2}$, but once again as soon as $m > 0$ the frequency dependence begins a transition to $f^{1-m/2}$ which is complete by $m \approx 0.02$.

The asymptotics of Eq. (21) indicate that in both high and low frequency limits, the intergranular friction is the dominant loss mechanism, while from Fig. 3 both mechanisms play important roles in the mid-frequency range. This is similar to the results of Biot-Stoll theory. Brunson has shown that Biot theory with complex shear moduli is able to account for details of the measured attenuation, specifically the "knee" in Fig. 6 of Ref. 22 that a linear fit would miss. (See also Fig. 1 of Ref. 3 for further deviations from the f^1 dependence for shear attenuation.) From the similarities in the behavior of the Biot-Buckingham and Biot-Stoll theories in Fig. 3 it seems that Biot-Buckingham theory would also be able to capture these details in the attenuation. A true test, as seen in Fig. 3(a) would be a measurement of the shear speed across a large frequency range, however this measurement may be prohibitively difficult in sandy sediments.

Using the values for the shear rigidity coefficient and the corresponding material exponent, the remaining coefficient and exponent can be determined for the compressional wave through a best fit to the data. This approach differs from Buckingham's development of his model where he assumes that the material exponents should be equal to one another⁴. In his model, the grain-to-grain friction is due to a number of random micro-asperity sliding

events, each of one which is assumed to be identical regardless of whether the grain-to-grain motion is radial or compressional. Since the material exponents characterize these individual events, it seems reasonable that they should have the same values. Buckingham presents limited evidence in the form of data-model comparisons that support this conclusion for his model. The data-model comparisons presented here support the conclusion that n and m are not equal, hence they are treated separately.

The compressional sound speed and attenuation predicted by the Biot-Buckingham model for the SAX99 sediment are presented in Fig. 4(a) and (d). Both n and γ_p were determined from a best fit to the data and were found to be $n = 1.088$ and $\gamma_p = 41.96$ Pa. This hybrid model succeeds in combining the strengths of both the Biot and Buckingham models and follows the data better than either individual model. The model also contradicts Buckingham's conclusions about the importance of losses due to viscous flow for the compressional wave. Whereas he concludes that viscous loss is the dominant mechanism at high frequencies, the Biot-Buckingham model predicts that viscous loss dominates in the mid-frequencies while granular friction is the dominant mechanism at high and low frequencies. This is similar to the asymptotics of the shear wave where granular friction also dominates at both the high and low frequencies. An analysis of the asymptotics of the compressional wave are not as straightforward as for the shear wave, but there are several observations which can be made immediately. Since the frequency dependence of the frame bulk modulus is nearly linear, for low frequencies granular friction will dominate the attenuation since the attenuation due to viscous flow goes as f^2 . In the high frequency limit, $K_b(\omega)$ becomes very large and hence dominates the wave propagation.

In order to compare the Biot-Buckingham model to the data from the glass bead sediments, four variables need to be determined: n , m , γ_p , and γ_s . Unlike the SAX99 data there are no shear wave measurements to use to determine the shear rigidity coefficient and exponent. The results for the SAX99 data, however, suggest that the shear modulus may be negligible compared to the other moduli. Setting $\mu_b = 0$ for the Biot-Buckingham model yields both sound speed and attenuation predictions that are nearly indistinguishable from the EDFM predictions. Consequently, for the glass bead sediments, the shear rigidity coefficient is taken as $\gamma_s = 0$. The predictions of the Biot-Buckingham model are

shown in Fig. 4(b) and (e) for the water and glass bead sediment and in Fig. 4(c) and (f) for the silicone oil and glass bead sediments.

For water and glass beads, the grain-to-grain shearing parameters were determined to be $n = 0.915$ and $\gamma_p = 182.94$ Pa. The predictions match the data well in this case, but it is difficult to say whether or not it does any better than the Buckingham model over this limited frequency range. For the silicone oil and glass beads, the grain-to-grain shearing parameters were determined to be $n = 1.059$ and $\gamma_p = 57.89$ Pa. The Biot-Buckingham model captures the data very well in this case and with values for the grain-to-grain parameters that are consistent with the other sediments. This differs from the Buckingham model for which the material exponent increases by a factor of 10 relative the water/glass bead sediment. This indicates that for the Buckingham model the increase in attenuation and dispersion must be due to a *decrease* in the strain-hardening at the micro-asperities even though the viscosity of the pore fluid was increased by a factor of 100. In the Biot-Buckingham model, the increase in attenuation is due to the increase in the viscosity of the pore fluid, while the attenuation due to the grain-to-grain friction is nearly identical to that observed in the previous glass bead sediment and in the SAX99 sediment.

Not only are the grain-to-grain shearing parameters similar in all three sediments, but the material exponent is very nearly equal to one, as can be seen in Table II. This suggests that the Biot-Buckingham model with $n = 1$ may yield predictions that compare favorably to the data. The results of the Biot-Buckingham model with $n = 1$ and γ_p taken as the free parameter, are shown as the dashed lines in Fig. 4. For the attenuation, the two curves are practically indistinguishable while for the sound speeds the deviation is most pronounced at high frequencies where the grain-to-grain losses are greatest. Even with this deviation, the model still compares favorably to the data.

V. DISCUSSION

The success of the Biot-Buckingham model with $n = 1$ has implications for the theoretical framework of the grain-to-grain shearing mechanism that Buckingham develops in Ref. 4. The material exponent is defined as $n = E_p/\theta_p$, where E_p is the elastic response

of the micro-asperity contact and θ_p reflects the nonlinear response of the viscous damping at the contact. Thus $n = 1$ means that elastic and viscous response is equal. This unlikely equality brings Buckingham's theoretical framework into question and suggests that another explanation for the form of Eq. 16 may be needed.

From a purely phenomenological standpoint, the complex moduli can be constructed from simple elastic and viscous elements. Consider the form of the bulk modulus in the Biot-Buckingham model when $n = 1$,

$$K_b(\omega) = -i\gamma_p\omega. \quad (26)$$

The modulus is purely imaginary and corresponds to a viscoelastic model composed entirely of dashpots. In Biot's phenomenological viscoelastic model, he suggests a viscoelastic modulus of the form,

$$K_b(\omega) = a(-i\omega)^s + K_b, \quad (27)$$

which, for $s = 1$, corresponds to the modulus in Eq. 26 in series with a real elastic modulus. For small values of this elastic term, the results of using Eq. 27 will not differ significantly from the predictions shown in Fig. 4.

Biot suggests several other expressions for the viscoelastic behavior of the moduli and suggests some possible mechanisms which might lead to viscoelasticity in porous media. Among these mechanisms, he suggests that dissipation may be present at the granular contacts due the viscous flow of fluid being squeezed in and out of the contact region. Biot constructs a simple spring and dashpot model of this squeeze flow but he is quick to recognize that this simple model is deficient. The viscous response of the fluid at the scales of the intergranular gaps differs considerably from the response of the bulk fluid. Subsequent work in tribology supports this conclusion and Buckingham's model is the first to try to capture this complex fluid-solid interaction at the grain contacts.

Although it is not possible to draw any conclusions from the theoretical implications of the data-model comparisons, the fits of the Biot-Buckingham model do provide some insight into the nature of the attenuation mechanisms. The increase in the attenuation when the pore fluid is changed from water to silicone oil is captured by Biot theory indicating that viscous flow is an important contributor to the acoustic loss. For a viscosity increase of two orders of magnitude, the rigidity coefficient doubles as seen in Table II for $n = 1$.

The deviation of the rigidity coefficient for the SAX99 sediment from this simple viscosity dependence suggests that the attenuation mechanism may depend in a complex way on the other properties of the sand grain such as the surface roughness of the grain.

The discussion here has focused mainly on intergranular dissipation as the possible explanation for the deviation of the attenuation from the predictions of Biot theory. The initial hypothesis was that scattering was responsible for the losses observed in the SAX99 data. Although the measurements in glass beads suggest that the excess attenuation is not due to scattering, there is still evidence of scattering in the SAX99 data that remains to be addressed. The transmitted waveforms in the sediment show significant distortion and degradation as they propagate and potential scatterers are known to be present in the sediment¹². This kind of signal degradation was not observed in the glass bead sediments suggesting that scattering may still be a contributor to the acoustic attenuation in real sediments. The measurements presented here do suggest, though, that it may not be the sole or dominant attenuation mechanism at high frequencies and that a mechanism more fundamental to the nature of unconsolidated porous media needs to be taken into account. Whether these losses are related to grain-to-grain interactions or to some other mechanism, such as acoustic interactions with "force chains," remains an open question for further research and speculation.

-
- ¹ E.L. Hamilton, "Geoacoustic modeling of the sea floor," *J. Acoust. Soc. Am.* **68**, 1313-1340 (1980).
 - ² M.J. Buckingham, "Theory of acoustic attenuation, dispersion, and pulse propagation in unconsolidated granular materials including marine sediments," *J. Acoust. Soc. Am.* **102**, 2579-2596 (1997).
 - ³ M.J. Buckingham, "Theory of compressional and shear waves in fluid-like marine sediments," *J. Acoust. Soc. Am.* **103**, 288-299 (1998).
 - ⁴ M.J. Buckingham, "Wave propagation, stress relaxation, and grain-to-grain shearing in saturated, unconsolidated marine sediments," *J. Acoust. Soc. Am.* **108**, 2796-2815 (2000).
 - ⁵ A.C. Kibblewhite, "Attenuation of sound in marine sediments: A review with emphasis on

- new low-frequency data," J. Acoust. Soc. Am. **86**, 716-738 (1989).
- ⁶ M.A. Biot, "Generalized theory of acoustic propagation in porous dissipative media," J. Acoust. Soc. Am. **34**, 1254-1264 (1962).
 - ⁷ M.A. Biot, "Mechanics of deformation and acoustic propagation in porous media," J. Appl. Phys. **33**, 1482-1492 (1962).
 - ⁸ R.D. Stoll, "Marine Sediment Acoustics," J. Acoust. Soc. Am. **77**, 1789-1799 (1985).
 - ⁹ R.D. Stoll, *Sediment Acoustics, Lecture Notes on Earth Sciences* (Springer-Verlag, Berlin 1989).
 - ¹⁰ E.I. Thorsos, K.L. Williams, N.P. Chotiros, J.T. Christoff, K.W. Commander, C.F. Greenlaw, D.V. Holliday, D.R. Jackson, J.L. Lopes, D.E. McGehee, J.E. Piper, M.D. Richardson, and D.J. Tang, "An Overview of SAX99: Acoustic Measurements," IEEE J. Ocean. Eng., **26**, 4-25 (2001).
 - ¹¹ M.D. Richardson, K.B. Briggs, L.D. Bibee, P.A. Jumars, W.B. Sawyers, D.B. Albert, R.H. Bennett, T.K. Berger, M.J. Buckingham, N.P. Chotiros, P.H. Dahl, N.T. Dewitt, P. Fleischer, R. Flood, C.F. Greenlaw, D.V. Holliday, M.H. Hulbert, M.P. Hutnak, P.D. Jackson, J.S. Jaffe, H.P. Johnson, D.L. Lavoie, A.P. Lyons, C.S. Martens, D.E. McGehee, K.D. Moore, T.H. Orsi, J.N. Piper, R.I. Ray, A.H. Reed, R.F.L. Self, J.L. Schmidt, S.G. Schock, F. Simonet, R.D. Stoll, D.J. Tang, D.E. Thistle, E.I. Thorsos, D.J. Walter, and R.A. Wheatcroft, "An overview of SAX99: Environmental considerations," IEEE J. Ocean. Eng. **26**, 26-54 (2001).
 - ¹² K.L. Williams, D.R. Jackson, E.I. Thorsos, D.J. Tang, and S.G. Schock, "Comparison of sound speed and attenuation measured in a sandy sediment to predictions based on the Biot theory of porous media," IEEE J. Ocean. Eng. **27**, 413-428 (2002).
 - ¹³ P.K. Seifert, B. Kaelin and L.R. Johnson, "Effect on ultrasonic signals of viscous pore fluids in unconsolidated sand," J. Acoust. Soc. Am. **106**, 3089-3094 (1999).
 - ¹⁴ F.P. Bowden and D. Tabor, *Friction and Lubrication of Solids* (Oxford University Press, 2000)
 - ¹⁵ J. Bear, *Dynamics of Fluids in Porous Media* (Dover Publications, New York, 1988) p. 166.
 - ¹⁶ J.G. Berryman, "Effective conductivity by fluid analogy for a porous insulator filled with a conductor," Phys. Rev. B. **27**, 7789-7792 (1983).

- ¹⁷ J.G. Berryman, "Confirmation of Biot's theory," Appl. Phys. Lett. **34**, 382-384 (1980).
- ¹⁸ M.J. Buckingham and M.D. Richardson, "On tone-burst measurements of sound speed and attenuation in sandy marine sediments," IEEE J. Ocean. Eng. **27**, 429-454 (2002).
- ¹⁹ K.L. Williams, "An effective density fluid model for acoustic propagation in sediments derived from Biot theory," J. Acoust. Soc. Am. **110**, 2276-2281 (2001).
- ²⁰ E. Kjartansson, "Constant Q-wave propagation and attenuation," J. Geophys. Res. **84**, 4737-4748 (1979).
- ²¹ A. Turgut, "An investigation of causality for Biot models by using Kramers-Krönig relations," in *Shear Waves in Marine Sediments* ed. by J.M. Hovem, M.D. Richardson, and R.D. Stoll (Kluwer, Dordrecht, 1991), pp. 295-304.
- ²² B. Brunson and R. Johnson, "Laboratory measurements of shear wave attenuation in saturated sand," J. Acoust. Soc. Am. **68**, 1371-1375 (1980).

TABLE I: Parameters used in calculating the effective density fluid model and Buckingham model results. The Biot-Buckingham model results were also calculated using these results except for the material exponent and rigidity coefficient.

| Parameter | Value | | |
|--|--------------------------------------|--------------------------------------|---------------------------------------|
| | SAX99 | Water/Beads | Si100/Beads |
| Bulk modulus of grains or glass beads (K_g) | 3.2×10^{10} Pa | 7.0×10^{10} Pa | 7.0×10^{10} Pa |
| Mass density of grains or glass beads (ρ_g) | 2690 kg/m ³ | 2500 kg/m ³ | 2500 kg/m ³ |
| Bulk modulus of pore fluid (K_f) | 2.395×10^9 Pa | 2.23×10^9 Pa | 9.68×10^8 Pa |
| Mass density of pore fluid (ρ_f) | 1023 kg/m ³ | 1000 kg/m ³ | 968 kg/m ³ |
| Viscosity of pore fluid (ν) | 0.00105 kg/m·s | 0.001 kg/m·s | 0.096 kg/m·s |
| Porosity (β) | 0.385 | 0.384 | 0.36 |
| Permeability (κ) | 2.5×10^{-11} m ² | 1.1×10^{-10} m ² | 8.43×10^{-11} m ² |
| Tortuosity (α) | 1.35 | 1.45 | 1.47 |
| Material exponent ($n = m$) | 0.0901 | 0.0467 | 0.3902 |
| Rigidity coefficient ($\gamma_T = \gamma_P + (4/3)\gamma_S$) | 2.6823×10^8 Pa | 3.871×10^8 | 1.472×10^6 Pa |

TABLE II: Material exponents and compressional rigidity coefficients used in the Biot-Buckingham model for each sediment. The parameters were determined from a fit to the data allowing both parameters to be free in the first case and fixing $n = 1$ in the second case.

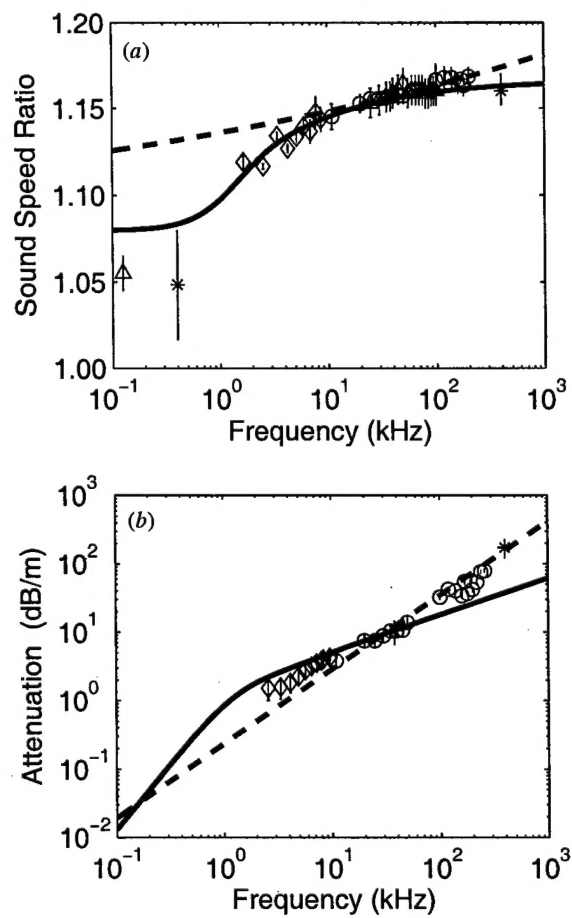
| Sediment | Fit with two free parameters | | Fit with one free parameter | |
|-------------------|------------------------------|------------|-----------------------------|------------|
| | n | γ_p | n | γ_p |
| SAX99 | 1.088 | 41.96 Pa | 1.00 | 146.82 Pa |
| Water/Glass Beads | 0.915 | 182.94 Pa | 1.00 | 54.79 Pa |
| Si100/Glass Beads | 1.059 | 57.89 Pa | 1.00 | 115.55 Pa |

FIG. 1: (a) Sound speed and (b) attenuation measured during SAX99. Details of these measurements can be found in Ref. 12. Also shown are the sound speed and attenuation predictions for Biot Theory (solid line) and the Buckingham model (dashed line) using the parameters given in Table I.

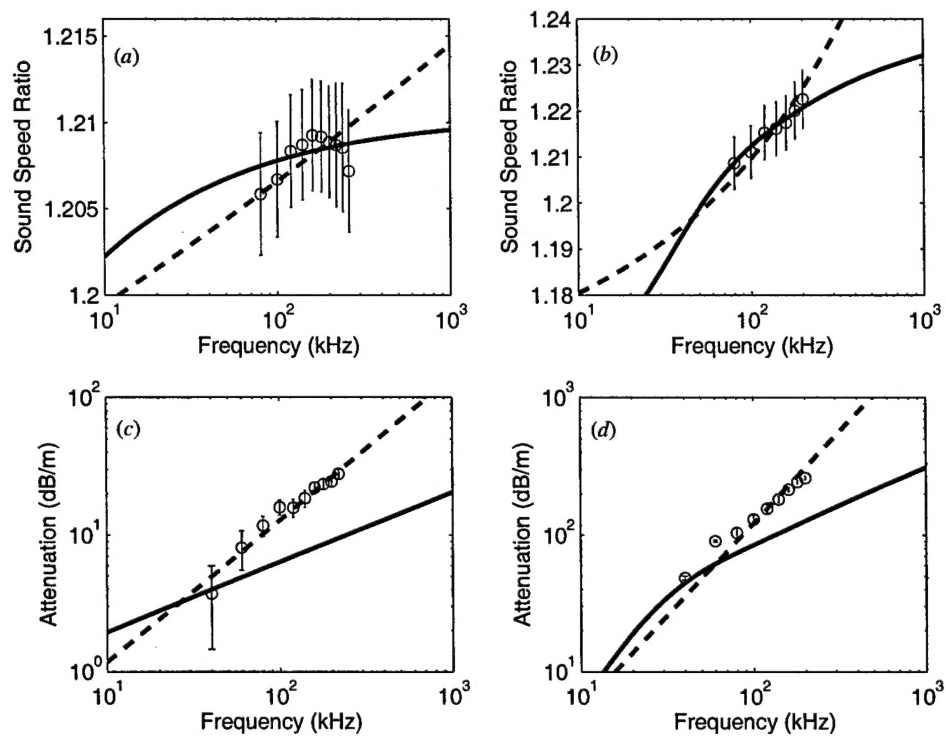
FIG. 2: Sound speed measurements made in a glass bead sediment saturated with (a) water and (b) silicone oil. Attenuation measurements made in a glass bead sediment saturated with (c) water and (d) silicone oil. Also shown are the predictions of the EDFM (solid line) and the Buckingham model (dashed line) using the parameters given in Table I. The error bars on the data points represent uncertainties in the position of the hydrophones as well as the distribution of multiple measurements in each sediment.

FIG. 3: (a) Shear wave speed and (b) attenuation. The data point at 1 kHz is a shear wave measurement made during SAX99 by Richardson¹¹. The shear wave speed and attenuation predicted by Biot Theory (dashed line), the Buckingham model (dotted line), and the Biot-Buckingham model (solid line). Each of these models was fit to the data point.

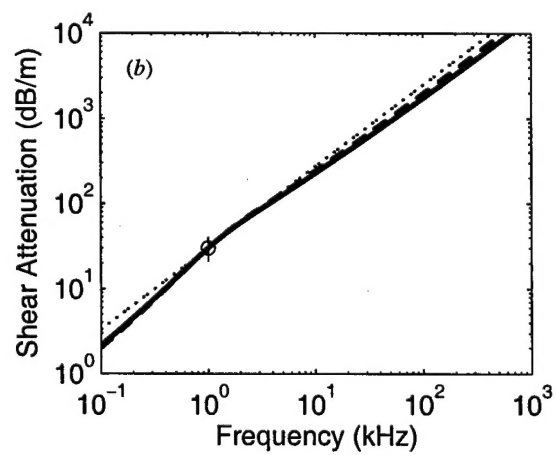
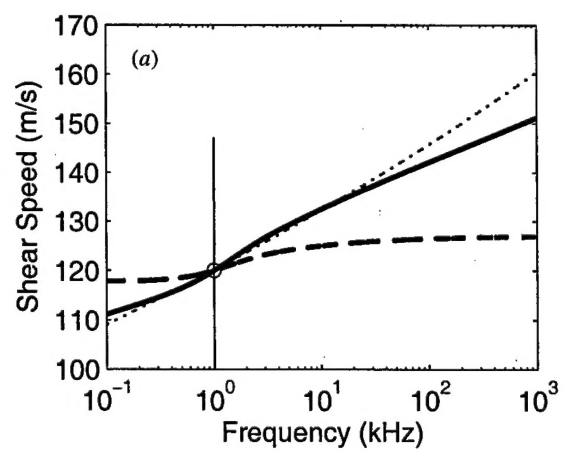
FIG. 4: (a-c) Sound speed and (d-f) attenuation predictions using the Biot-Buckingham model for the sediment at SAX99, the water and glass bead sediment, and the silicone oil and glass bead sediment. The grain-to-grain shearing parameters in the Biot-Buckingham model were determined in two ways. For the solid line, the values of both the compressional rigidity coefficient, γ_p , and the material exponent, n , which gave the best fit to both the sound speed and attenuation data were found. For the dashed line, the material exponent was set to $n = 1$ while the value of γ_p was determined from the best fit.



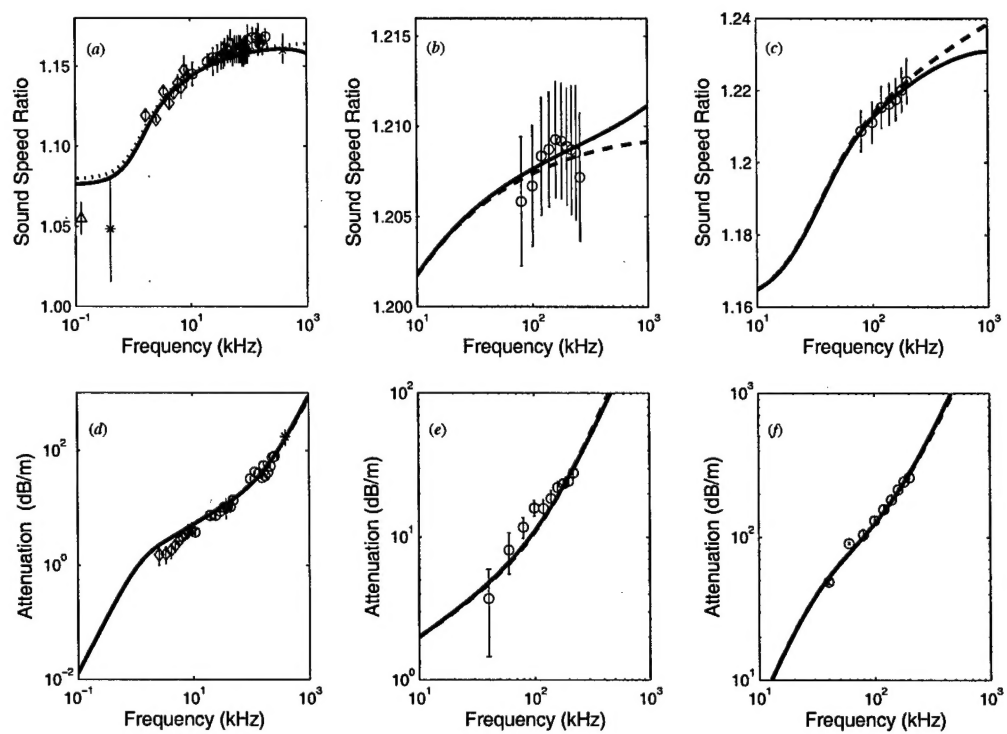
Hefner and Williams, Fig. 1



Hefner and Williams, Fig. 2



Hefner and Williams, Fig. 3



Hefner and Williams, Fig. 4